An Extension of the Marcus Equation for Atom Transfer Reactions

Paul Blowers and Richard I. Masel*

Department of Chemical Engineering, University of Illinois at Urbana−Champaign, Urbana, Illinois 61801-3792

Received: January 4, 1999; In Final Form: July 2, 1999

The Marcus equation for electron transfer has been widely applied to atom transfer reactions, but the equation does not seem to work well for very endothermic or very exothermic reactions. In this paper, a modified model is proposed. The modified model assumes that the potential energy surface can be written as a sum of the potentials for the individual molecules and an intermolecular potential that keeps the reactants apart. The activation barrier predicted by the model is within 3 kcal/mol of that predicted by the Marcus electron transfer equation when $-1 \leq \Delta H_r/4E_a^\circ \leq 1$, where ΔH_r is the heat of reaction and E_a° is the intrinsic barrier. However, there are significant deviations when $\Delta H_r/4E_a^\circ < -1$ and when $\Delta H_r/4E_a^\circ > 1$. The modified model predicts that the activation barrier should equal $\Delta H_r/4E_a^\circ$ in the very endothermic limit, (i.e., $\Delta H_r/4E_a^\circ > 1$), while the Marcus electron transfer equation predicts that the activation energy, E_a, should diverge from ΔH_r. Data shows that E_a approaches ΔH_r. The modified model predicts that the activation barrier goes to zero for very exothermic reactions, (i.e., $\Delta H_r/E_a^\circ < -1$) while the Marcus electron transfer equation predicts large barriers. Data shows, though, that the barriers approach zero. We also compare to the Marcus hyperbolic cosine expression and find that the modified model is within 3 kcal/mol of the Marcus hyperbolic cosine expression over the entire energy range. The modified model predicts that the barriers to reaction are associated with Pauli repulsions and not with bond stretching. That prediction agrees with recent ab initio calculations, and the VB model but not with the intersecting parabola model. Overall, the modified model seems to extend the original Marcus equation to very endothermic and very exothermic reactions. Also, it gives predictions similar to the Marcus hyperbolic cosine expression over the entire energy range.

I. Introduction

Several years ago, Marcus[1,2] derived what is now called the Marcus equation to relate the heat of reaction, ΔH_r, to the activation barrier, E_a, for electron transfer reactions:

$$E_a = E_a^\circ\left(1 + \frac{\Delta H_r}{4E_a^\circ}\right)^2 \tag{1}$$

where E_a° is a constant. Murdoch[3−5] and Shaik et al.[6] also showed that the position of the transition state, $\chi^\ddagger$, is given by

$$\chi^\ddagger = 0.5 + \frac{\Delta H_r}{8E_a^\circ} \tag{2}$$

Equation 1 has been widely applied to electron transfer reactions and generally fits the data quite well. In electron transfer reactions, one often observes inverted behavior, as expected from the Marcus equation. Marcus inverted behavior is also often seen in intermolecular energy transfer rates and other de-excitation processes.

Given the success of the Marcus equation for electron transfer and energy transfer reactions, many investigators have tried to extend the results to atom transfer reactions. Murdoch,[3−5] Sutin et al.,[7,8] Jensen,[9] and Albery et al.[10,11] derived an analogue of the Marcus equation based on the curve-crossing model of Polanyi and Evans.[12] The idea is that the system goes up a potential energy contour and then down again, as indicated in Figure 1. If one assumes parabolic potentials, one can derive eqs 1 and 2. Marcus[2,13] pointed out that this approximation for atom transfer reactions is probably in error and derived an alternative equation for atom transfer.

$$E_a = E_a^\circ + \frac{1}{2}\Delta H_r + \frac{E_a^\circ}{\mathrm{Ln}\ 2}\mathrm{Ln}\left(\cosh\left(\frac{\Delta H}{2E_a^\circ}\mathrm{Ln}2\right)\right) \tag{3}$$

Nevertheless, eq 1 is often used for atom transfer reactions. Guthrie[14] has also proposed a multidimensional extension of eq 1. The details are different, but the results are qualitatively the same.

Experimentally, though, atom transfer reactions look different than electron transfer reactions. It is unusual to observe Marcus inverted behavior in atom transfer reactions. For example, Westley[15] has an extensive table of activation barriers for reactions of interest to combustion. Figure 2 is a plot of the activation barriers versus the heat of reaction for 478 open-shell radical exchange reactions of the form:

$$\mathrm{R{-}H} + \mathrm{R}^1 \rightarrow \mathrm{R} + \mathrm{H{-}R}^1 \tag{4}$$

The actual reactions are listed in the Supporting Information. The predictions of the Marcus equation are included for comparison. In the Marcus plot, we used a single value of E_a°, but in reality, the intrinsic barriers as estimated from identity reactions vary from 7 to 12 kcal. We used the average value of E_a^o to generate a single Marcus plot.

The data shows that E_a approaches zero when ΔH_r is less than −20 kcal/mol, E_a approaches ΔH_r when ΔH_r is greater

* To whom correspondence should be addressed

10.1021/jp990039u CCC: $18.00
Published on Web 08/13/1999

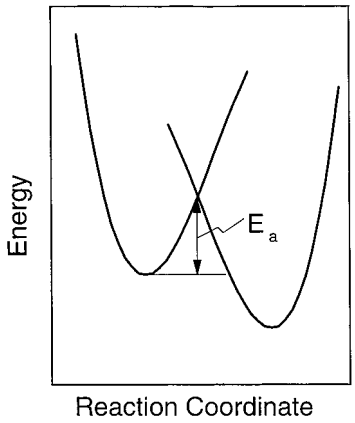

Figure 1. Changes in energy as reaction proceeds according to the curve-crossing model.

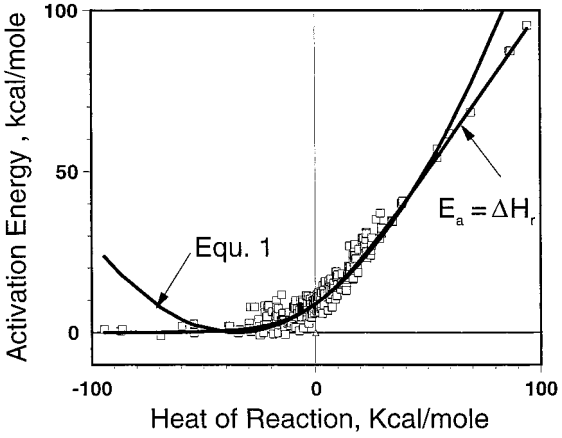

Figure 2. Activation barriers for 478 reactions of the form R−H + R′ → R + H−R′. Results of Westly.[15] The predictions of eq 1 with $E_a° = 9$ kcal/mol are included for comparison.

than 50 kcal/mol, and E_a varies smoothly in between. In contrast, the Marcus electron transfer equation predicts that E_a grows to infinity as ΔH_r approaches $-\infty$. Further, the Marcus electron-transfer equation predicts that E_a diverges from ΔH_r when ΔH_r grows to $+\infty$. If we expand our search and consider all of the reactions in the compendiums of Westley,[15] Benson,[16] and Kondrat'ev,[17] we find that there are no highly exothermic reactions listed in these compendia with large activation barriers. While it is theoretically possible for an exothermic atom transfer reaction to have a large barrier due to a steric repulsion, the number of examples in the literature is small. E_a approaches ΔH_r for large endothermic values of ΔH_r in all of the data in Figure 2 and all of the other data in Westley et al.,[15] Benson,[16] and Kondrat'ev.[15] However, eq 1 predicts that E_a diverges from ΔH_r at large ΔH_r.

Equation 3 does go to the correct result in the limit of very endothermic and very exothermic reactions. However, it has not been extensively used in the literature.

Another weakness is that eq 2 does not correctly predict the position of the transition state. For example, Figure 3 compares Lee and Masel's[18,19] ab initio calculations of $\chi^‡$ to those predicted from eq 2 for a series of reactions of the form

$$H + CH_3R \rightarrow CH_4 + R \tag{5}$$

Notice that there is little agreement between the predictions of eq 2 and the ab initio calculations.

Such a result is not surprising. The Marcus equation was originally derived for electron transfer reactions. Cohen and

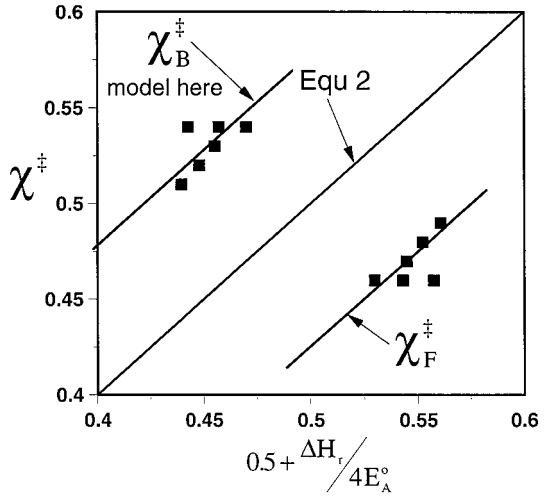

Figure 3. Comparison of the position of the transition state predicted by eq 2 to Lee and Masel's G-2[18,19] calculations for a number of reactions of the form $H + CH_3R \rightarrow CH_4 + R$ with R = CH_3, C_2H_5, CH_2CF_3, CH_2CN, $CH_2C_2H_5$.

Marcus[13] examined the application of the Marcus equation to atom transfer reactions. They found that the Marcus equation works when $-4E_a° < \Delta H_r < 4E_a°$, but the assumptions in the equation fail in cases where $-4E_a° > \Delta H_r$ or $4E_a° < \Delta H_r$ (i.e., very exothermic of very endothermic reactions). Cohen and Marcus suggested that eq 3 would work much better for atom transfer reactions. However, eq 3 has not been extensively cited in the literature.

The object of this paper is to find a modified equation that extends the original Marcus equation to very endothermic or very exothermic reactions. Our approach will be to build on some work Polanyi et al.[20−23] did years ago to understand the potential energy surfaces for chemical reactions which has been expanded by many subsequent investigators. The method starts by writing $V(\bar{R})$, the potential energy surface for the reaction A + BC → AB + C as

$$V(\bar{R}) = V_{AB} + V_{BC} + V_I \tag{6}$$

where V_{AB} is the potential energy surface for an AB molecule in the absence of C, V_{BC} is the potential energy surface for a BC molecule in the absence of A, and V_I is an interaction energy. Kuntz et al.[23] proposed that one could simplify eq 6 by averaging the potentials over all of the internal coordinates and only examining the bonds that break and form. According to Kuntz et al., the potential energy surface, V, for a simple atom transfer reaction can be written as a sum of V_B, the potential for the bond that breaks, V_F the potential for the bonds that form, and V_r, the intermolecular potential between the reactants.

$$V(r_F,r_B) = V_F(r_F) + V_B(r_B) + V_r(r_F,r_B) \tag{7}$$

In eq 7, the subscript F refers to the bond that forms during the reaction (i.e., the R−H bond in reaction 4), while the subscript B refers to the bond that breaks during the reaction, and r_F and r_B are the lengths of the bonds that form and break.

In this paper, we use eq 7 to derive a simple approximation for the position and energy of the transition state. Our approach will follow closely Murdoch's[3−5] derivation of the Marcus equation. We will fit empirical forms to V_F, V_B, and V_r and then use the results to derive an expression for the activation barrier and the position of the transition state. We will then compare the approximation to ab initio calculations of the

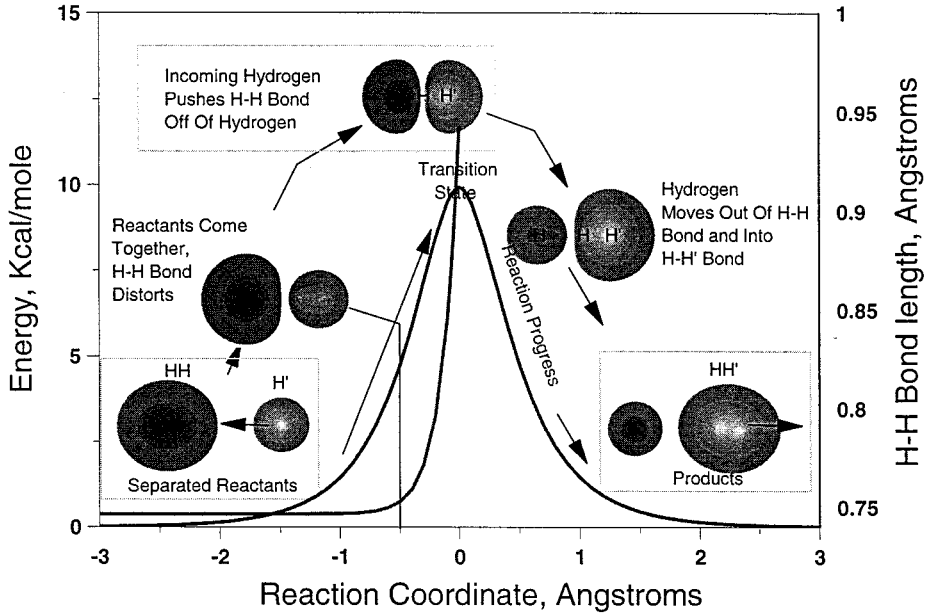

Figure 4. Orbital pictures for $H' + H_2 \rightarrow H'H + H$ along the reaction coordinate. The energies and bond lengths are calculated at the CCSD-(T)/6-311++G(3df, 3pd) level.

transition state position and energy for a variety of reactions, and to data for the variation of E_a with heat of reaction.

II. The Potential

First, we need to get some approximations to V_F, V_B, and V_r. In a recent paper,[18] we have fit equations to our potential energy surfaces for several reactions of the form in eq 4. We find that we can fit the ab initio calculations to the model if we assume that V_F and V_B are the energy to stretch bonds and V_r is associated with the Pauli repulsions to bring the reactants close together.

According to our ab initio calculations[18,19,24−27] and work of previous investigators,[33,34,37] the Pauli repulsions between the electrons in the reactants play a significant role in the barrier to reaction. For example, Figure 4 shows a plot of the orbital distortions that occur during the reaction $H + H_2 \rightarrow H_2 + H$ calculated as described in our recent work.[18,19] Notice that, as the reaction occurs, the orbitals on the hydrogen and H_2 distort. The orbital distortions are associated with the Pauli repulsions that cause diffuse and polarization functions to mix with the ground state during reaction. According to our ab initio calculations[26,27] and Shaik's VB calculations,[33,34] the Pauli repulsions are the main reason for barriers in the reactions in Figure 2.

Bernstein and Muckerman[28] show that one can approximate the Pauli repulsions by

$$V_{Pauli} = V_0 \exp(-\alpha_3 r_F - \alpha_4 r_B) \tag{8}$$

where V_0, α_3, and α_4 are constants. We have calculated the potential for the interaction of a hydrogen atom with an ethane at the G-2 level. That potential also fits eq 8 at distances comparable to those in reactions.

In this paper, we will make the ad hoc assumption that $V_r = V_{Pauli}$. This assumption is not justified theoretically. In particular, previous investigators[35−38] have found that ionic structures are often important in transition states for reactions.

One would also expect that the form in eq 8 would not necessarily be applicable for the interaction of open-shell systems. However, the approach here is to make the assumption anyway, and see if a useful result is obtained.

An additional ad hoc assumption is that V_F and V_B are given by Morse potentials:

$$V_F = w_F\{\exp(\alpha_1(r_{F,equ} - r_F)) - 1\}^2 - w_F$$
$$V_B = w_B\{\exp(\alpha_2(r_{B,equ} - r_B)) - 1\}^2 \tag{9}$$

where w_F and w_B are the bond energies of the bonds that form and break during the reaction, r_F and r_B are the lengths of these bonds, $r_{B,equ}$ and $r_{F,equ}$ are the equilibrium bond lengths, and α_1 and α_2 are constants. Combining eqs 7−9 yields:

$$V(r_F,r_B) = w_F\{\exp(\alpha_1(r_{F,equ} - r_F)) - 1\}^2 - w_F + w_B\{\exp(\alpha_2(r_{B,equ} - r_B)) - 1\}^2 + V_0 \exp(-\alpha_3 r_F - \alpha_4 r_B) \tag{10}$$

Next, it is useful to derive an equation for the saddle point energy in eq 10. A detailed derivation is given in the Supporting Information. The result for the special case where $\alpha_1 = \alpha_3$ and $\alpha_2 = \alpha_4$ is

$$E^{\ddagger} = \begin{cases} 0 & \text{if } \dfrac{\Delta H_r}{4E_a^0} < -1 \\ \dfrac{(w_0 + 0.5\Delta H_r)(V_P - 2w_0 + \Delta H_r)^2}{((V_P)^2 - 4(w_0)^2 + (\Delta H_r)^2)} & \text{if } -1 \le \dfrac{\Delta H_r}{4E_a^\circ} \le 1 \\ \Delta H_r & \text{if } \dfrac{\Delta H_r}{4E_a^\circ} > 1 \end{cases} \tag{11}$$

where $E^{\ddagger}$, is the energy of the saddle point relative to the reactants, E_a° is intrinsic activation barrier for the reaction, ΔH_r is the heat of reaction, w_0 is the average bond energy, i.e.,

$$w_0 = (w_F + w_B)/2 \tag{12}$$

and V_P is the strength of the Pauli repulsions at the transition

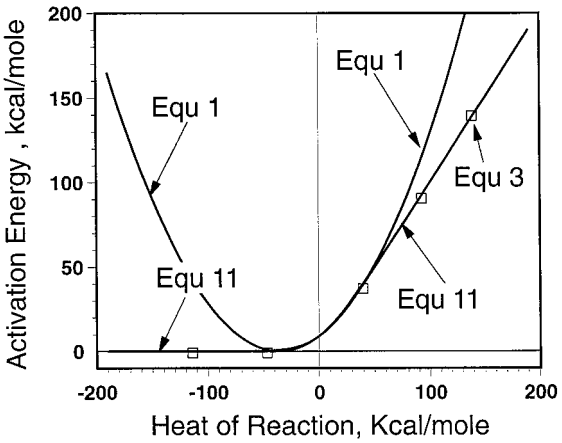

Figure 5. Plot of the height of the barrier $E^{\ddagger}$ as a function of the heat of reaction ΔH_r for an average bond strength, $w_0 = 110$ kcal/mol, $E_a^\circ = 9$ kcal/mol, and $\alpha_1 = \alpha_3$ and $\alpha_2 = \alpha_4$ compared to (a) the Marcus electron transfer and (b) eq 3.

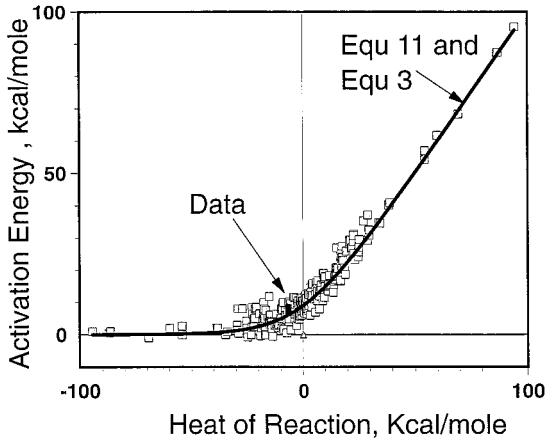

Figure 6. Comparison of the trends in Figure 5 to the data in Figure 2. The predictions of the Marcus equation for identical parameters are included in the comparisons.

state. For future reference, it is also important to note

$$V_P = 2w_0\left(\frac{w_0 + E_a^\circ}{w_0 - E_a^\circ}\right) \tag{13}$$

Equation 13 allows one to calculate V_P from E_a° estimated via identity reactions.

Later in the paper, we will also need a few other variables. First, it is useful to also define $\chi_F^{\ddagger}$, the dimensionless position of the transition state for the forward reaction, by

$$\chi_F^{\ddagger} = \frac{n_F^{\ddagger}}{n_F^{\ddagger} + n_B^{\ddagger}} \tag{14}$$

where $n_F^{\ddagger}$ and $n_B^{\ddagger}$ are the Pauling bond orders for the forming and breaking bond at the transition state. It is also useful to define E_{bond}, the change in the total bond energy of the system in moving from the reactants to the transition state. Equations for $\chi_F^{\ddagger}$ and E_{bond} are given in the Supporting Information.

IV. Qualitative Features of the Model

Figure 5 is a plot of $E^{\ddagger}$ from eq 11 vs ΔH_r for some typical values of the parameters. According to the model, $E^{\ddagger}$ is zero for very exothermic reactions, approaches ΔH_r for very endothermic reactions, and varies smoothly in between. The model is virtually indistinguishable from the Marcus electron transfer equation when -36 kcal/mol $\leq \Delta H_r \leq 36$ kcal/mol, i.e., when $-1 \leq \Delta H_r/4E_a^\circ \leq 1$. However, there are differences for very exothermic and very endothermic reactions. The Marcus electron transfer equation predicts that very endothermic reactions should have large activation barriers. However, the model here predicts that the barrier should approach zero. Also, the Marcus electron transfer equation predicts that E_A grows parabolically with ΔH_r at large ΔH_r. However, the model in this paper predicts that $E^{\ddagger} = \Delta H_r$ for very endothermic reactions instead.

Figure 5 also compares the predictions of eq 11 to those of eq 3, Marcus' hyperbolic cosine result. Notice that the activation barriers predicted by our equation are virtually identical to Marcus' hyperbolic cosine expression, even though the physics in our expression is different than that used to derive Marcus' result. This result indicates that the variation in the activation barrier is insensitive to the details of the model, and that makes the expressions very useful.

Figure 6 compares the predictions of eq 11 to the data in Figure 2. A line for eq 3 is also shown, although the line to eq 3 is indistinguishable from that for eq 11. As in Figure 2, we assume $E_a^\circ = 9$ kcal and $w_0 = 120$ kcal/mol. In reality, E_a° and w_0 will vary over the data set. However, we ignored the variations to keep everything compatible with Figure 2.

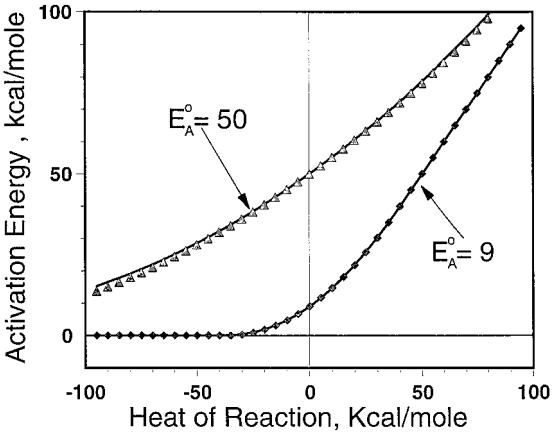

Figure 7. Variation in the activation energy calculated via eq 15 (points) and eq 11 (lines) for $w_0 = 120$ kcal/mol, $\alpha_1 = \alpha_3$ and $\alpha_2 = \alpha_4$ and various values of E_a°.

Notice that eq 11 follows the trends in the data much more closely than the Marcus electron transfer equation. $E^{\ddagger}$ varies linearly with ΔH_r at large ΔH_r, and $E^{\ddagger}$ is zero at low ΔH_r. There is no inverted region in either the data or the model.

Figure 7 compares the model here to a different empirical approximation.

$$E_a^{\ddagger} = \begin{cases} 0 & \text{for } \Delta H_r/4E_a^\circ < -1 \\ E_a^\circ\,(1 + \Delta H_r/4E_a^\circ)^2 & \text{for } -1 \leq \Delta H_r/4E_a^\circ \leq 1 \\ \Delta H_r & \text{for } \Delta H_r/4E_a^\circ > 1 \end{cases} \tag{15}$$

The lines in the figure are calculated via eq 11, while the points are calculated from eq 15. Equation 15 is not exact, but it does fit eq 11 to within 3 kcal/mol under all conditions we have examined. Consequently, it appears that the model here predicts activation barriers that are very similar to those from the Marcus electron transfer equation when $-1 \leq \Delta H_r/4E_a^\circ \leq 1$. Still, the predicted activation barriers are quite different than those predicted by the Marcus electron transfer equation when $\Delta H_r/4E_a^\circ$ is either less than -1 or greater than 1.

Figure 8 shows how the predictions of the model here change as we fix E_a° and vary w_0. There are six values of w_0 in the

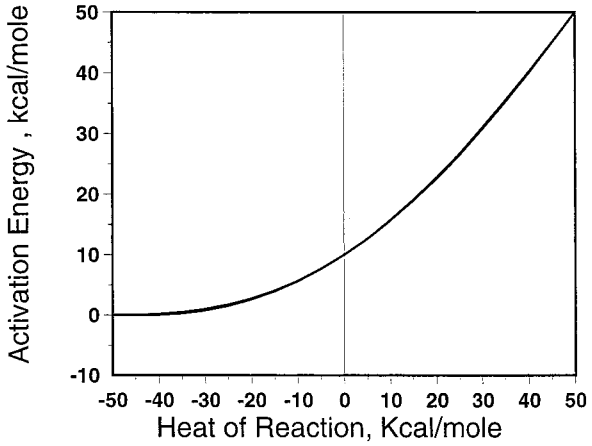

Figure 8. Variation in the activation energy with changing w_0 with $E_a^\circ = 9$ kcal/mol. The figure shows lines for $w_0 = 60$, 80, 100, 120, 140, and 160 kcal/mol.

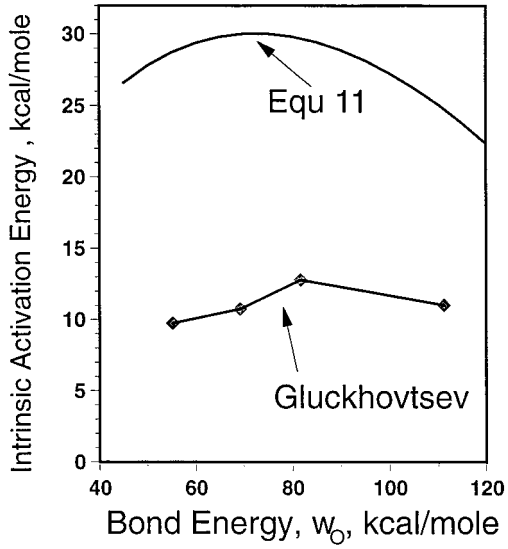

Figure 9. Variations in the height of the intrinsic barrier for a series of identity reactions as the average bond energy w_0 changes. We assumed that V_P is constant and allowed E_a° to vary.

figure, but the six plots differ by such a small amount that the various lines merge. Consequently, even though w_0 appears in our model, the predicted activation barriers are almost independent of w_0 over a wide range.

Variations in w_0 do, however, change the intrinsic barrier. Figure 9 shows a plot of the intrinsic activation barrier as a function of w_0 with $V_P = 400$ kcal/mol, $\alpha_1 = \alpha_3$, and $\alpha_2 = \alpha_4$. Notice that the intrinsic barrier to reaction increases, reaches a maximum, and then decreases again with increasing w_0. The implication of Figure 9 is that, under some circumstances, it costs less energy to break a strong bond than to break a weak bond. This trend is entirely different from the curve-crossing model. In the curve crossing model, E_A increases linearly with w_0.

Figure 9 also shows the results of Glukhovtsev et al.'s[30,31] ab initio calculations of the central barrier for the identity reactions:

$$X' + CH_3X \rightarrow XCH_3 + X' \quad \text{for} \quad X = F^-, Cl^-, Br^-, \text{and } I^- \quad (16)$$

Notice that the central barrier for reaction 16 increases before decreasing with increasing bond energy, in qualitative agreement

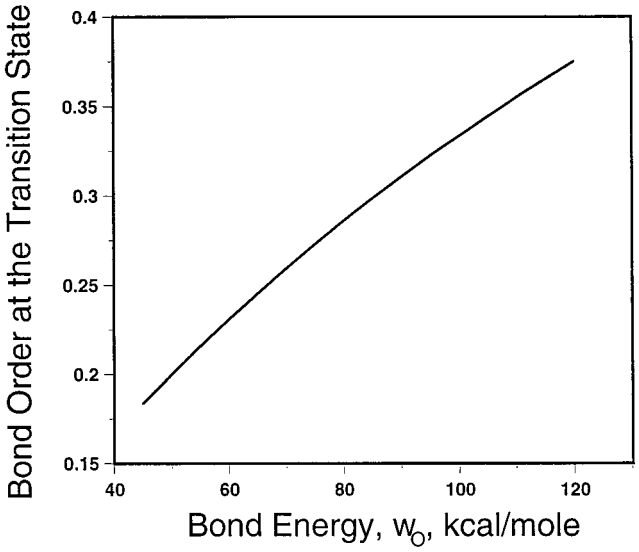

Figure 10. Variations in $n_B^\ddagger$ the bond order for the bond that breaks for the case in Figure 8.

with eq 11. Equation 11 does not fit exactly because the $X'CF_3X^-$ potential has a couloumbic attraction that is absent from eq 11. Still the qualitative trends from eq 11 are that there is a maximum in activation energy at intermediate bond strengths in agreement with Glukhovtsev's ab initio calculations for the reactions of the form in eq 16.

The decrease in E_a° with increasing bond energy occurs because the transition state gets tighter as w_0 increases. Figure 10 shows how $n_B^\ddagger$, the bond order of the breaking bond at the transition state, changes as w_0 increases. Notice that, when w_0 is small, the transition state is very extended (i.e., loose) so that bonds have to stretch significantly before the reaction occurs. However, as w_0 increases, the bond in the transition state shortens. It works out that more bond order is conserved at the transition state when w_0 is large rather than when it is small. The extra bond order causes the intrinsic activation energy to decrease in Figure 10.

Physically, the size of the transition state is determined by the ratio of the strength of the Pauli repulsion to the strength of the bond that breaks. As the Pauli repulsions increase, the transition state gets larger. As w_0 increases, it gets harder to stretch the bonds so the transition state distance decreases. According to the model here, the size of the transition state is determined by a balance between the bond energy and the Pauli repulsions. Strong bonds make the transition state tighter, which causes the drop in E_a° at large w_0 seen in Figure 9.

So far, we have assumed that V_p is a constant. In most chemical reactions, when you change the strength of the bonds, you also change the Pauli repulsions. Still, V_p can vary independently of the bond strength by careful substitutions in the reaction molecule. For example, if one replaces one of the methyl hydrogens in reaction 5 with a *tert*-butyl group, the Pauli repulsions will go up even though w_0 goes down. Therefore, one can sensibly discuss the idea that the Pauli repulsions can be varied independently of the bond strength.

Figure 11 is a plot of the intrinsic activation barrier, E_a°, as a function of V_p, the strength of the Pauli repulsions, with $\alpha_1 = \alpha_3$, $\alpha_2 = \alpha_4$, and $w_0 = 120$ kcal/mol. The intrinsic activation energy starts at 0 kcal/mol when $V_p = 0$. It stays at zero until $V_P = 240$ kcal/mol and then rises nonlinearly. The intrinsic activation barrier when $V_p = 600$ is 51.4 kcal/mol.

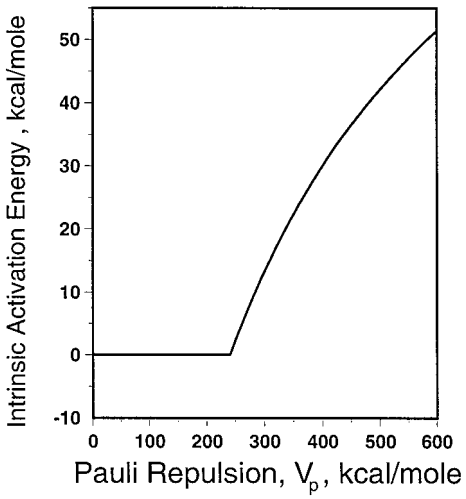

Figure 11. Variations in the intrinsic activation barrier, $E_a°$, as a function of the strength of the Pauli repulsion V_P, with $w_0 = 95$ kcal/mol; $\alpha_1 = \alpha_3$ and $\alpha_2 = \alpha_4$.

The $V_p = 0$ case may seem a little strange, but if there are no Pauli repulsions, then there will be nothing to keep the reactants apart. In that case, the reactants can form a stable complex. In this case there is no barrier to reaction.

One does not start to see an intrinsic barrier until the Pauli repulsion is stronger than the bond energy:

$$V_p > 2w_0 \tag{17}$$

so that no stable complex forms. At that point, there is a barrier to the reaction and the intrinsic activation barrier increases monotonically but nonlinearly as V_p increases.

Physically, increases in V_P correspond to increases in the steric repulsions. Consider the homologous series of reactions:

$$CH_3NO_2 + OH^- \rightarrow H_2O + (CH_2NO_2)^- \tag{18}$$

$$CH_3CH_2NO_2 + OH^- \rightarrow H_2O + (CH_3CHNO_2)^- \tag{19}$$

$$(CH_3)_2CHNO_2 + OH^- \rightarrow H_2O + ((CH_3)_2CNO_2)^- \tag{20}$$

where a proton is being transferred from nitromethane to a hydroxyl. As methyl groups are added to the carbon center, the steric repulsions increase. V_P also increases. We have calculated the activation energy for reactions 18−20 using a group additivity postulate and found that the activation barrier for eq 20 will be higher than the barrier for reaction 18, even though reaction 20 is more exothermic than reaction 18. Experimentally,[32] reaction 20 has a higher barrier than (18) even though $(CH_3)CHNO_2$ is a stronger acid than CH_3NO_2.

In the literature, people have considered reactions 18−20 anomalous because the rate decreases as the reaction becomes more exothermic; that is, the Brønsted slopes are negative.[32] The model here predicts negative Brønsted slopes, in agreement with the experimental data. Another feature of the model here is that it predicts a nonlinear Brønsted plot.

The nonlinearity in Figure 11 occurs because the bonds stretch to reduce the Pauli repulsions. Figure 12 shows how the Pauling bond order at the transition state changes as V_p increases. Notice that the Pauling bond order at the transition state decreases as the Pauli repulsions increase. According to the definition of the Pauling bond order, a decrease in the Pauling bond order at the transition state corresponds to a lengthening of the various bonds in the transition state. Therefore, the implication of Figure 12

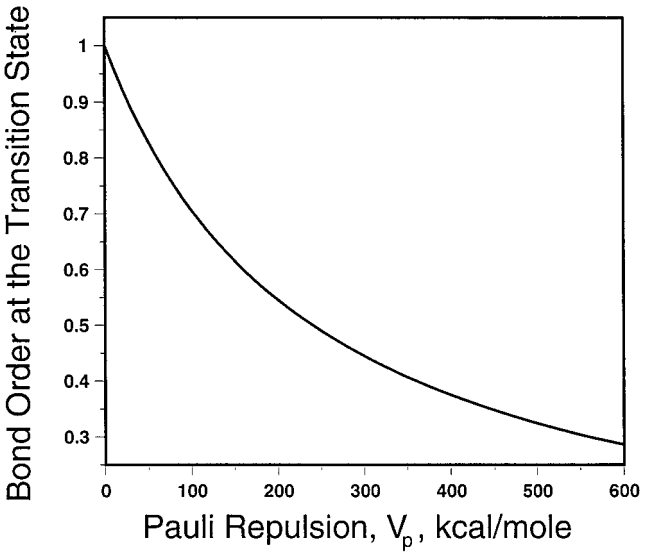

Figure 12. Variations in $n_B^‡$ the bond order at the transition state for the case in Figure 11.

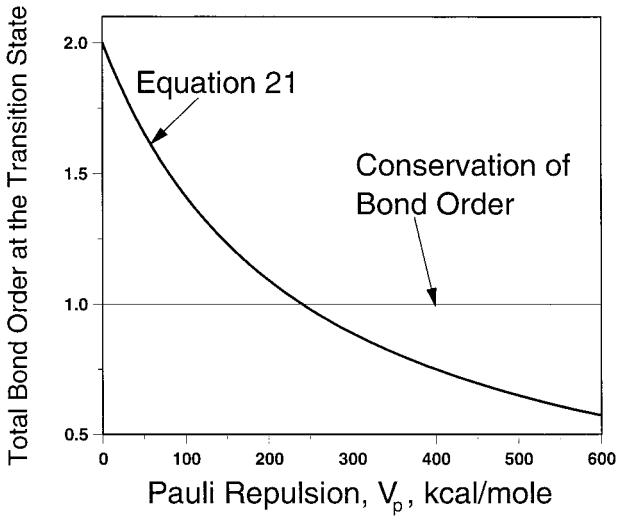

Figure 13. Variations in n_T, the total bond order of the system for the case in Figure 11.

is that the bonds are lengthening as the Pauli repulsions increase. Physically, as you increase the Pauli repulsions, the reactants are forced apart and the transition state becomes looser.

Another implication of the model is that the Pauling bond order is not conserved during the reaction. If bond order was conserved, then the total bond order, n_T, should be 1.0 everywhere along the intrinsic reaction pathway, where

$$n_T = n_F + n_D \tag{21}$$

Figure 13 shows a plot of n_T versus V_p. Notice that when $V_p = 0$, a stable complex forms and $n_F^‡ = n_D^‡ = 1$ or $n_T^‡ = 2.0$. As we increase the Pauli repulsions, the reactants are forced apart and $n_T^‡$ decreases. It happens that when $V_p = w_F + w_B$ the forces balance so that bond order is conserved (i.e., $n_T = 1$) over the reaction coordinate. However, the activation barrier is zero in such a case. When $V_p > w_F + w_B$, the total bond order at the transition state is less than 1 and Pauling bond order is not conserved. Here, there is also a finite barrier to reaction.

One might think that the barrier arises because the total bond order at the transition state is less than 1.0. However, Figure 14 shows how the total bond energy at the transition state, E_{bond},

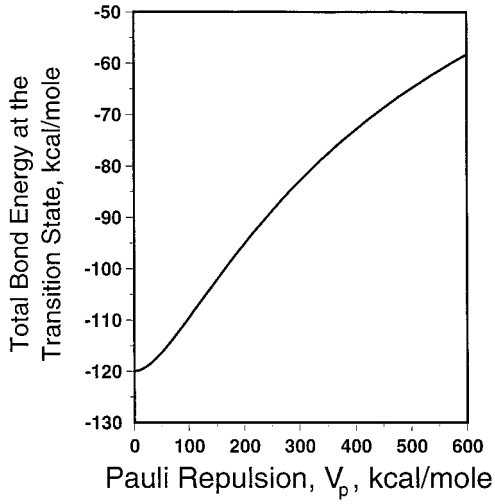

Figure 14. Total bond energy E_{tot} for the case in Figure 11.

varies as V_p changes. Notice that the total bond energy is negative over the entire range in the figure. A negative value of E_{bond} implies that the system gains more energy in partially forming a modified bond than it loses in partially breaking the original bond. As a result, bond extension does not produce a net barrier. According to the model here, the barriers to reaction arise because there are Pauli repulsions in getting the reactants close enough to react. Bond stretching lowers these barriers, which is the opposite effect compared to the intersecting parabola model.

V. Comparison to the Intersecting Parabola Model

It is useful to compare the results here to those from the intersecting parabola model.[3−11] The intersecting parabola model predicts Marcus-like behavior with an inverted region and a parabolic rise in energy with increasing ΔH. The data in Figure 2 does not show that trend. Instead, there is no inverted region and a linear variation of E_A with ΔH at large ΔH.

Physically, the intersecting parabola model predicts an inverted region because the model assumes that the size of the transition state is fixed. If you have a very exothermic reaction, you get a curve-crossing before the minimum in the reaction, as shown in Figure 15b, and that causes Marcus inverted behavior.

The model in section II does not allow this inverted behavior to occur. Instead, the transition state expands to give the situation in Figure 15b. There is no barrier to reaction under this situation.

A similar effect occurs for very endothermic reactions. When the reaction is very endothermic, the intersecting parabola model predicts that the intersection of the two curves will be past the product. However, the model here suggests that the transition will expand again to compensate these effects. In this case, $E_A = \Delta H_r$, and not $E_A > \Delta H_r$, as predicted by the intersecting parabola model.

Generally, unlike the intersecting parabola model, the model here predicts that the bonds can be extended if the bond extension lowers the barriers to reaction. The intersecting parabola model does not allow bonds to stretch, and so the intersecting parabola model gives the wrong behavior for ligand transfer reactions with large barriers.

In a more fundamental way, the model here differs from the intersecting parabola model in that it identifies the barriers to reaction with the Pauli repulsions between the reactants and not the energy to stretch bonds. In recent papers,[24−27] Blowers and Masel examined the activation barriers for another set of

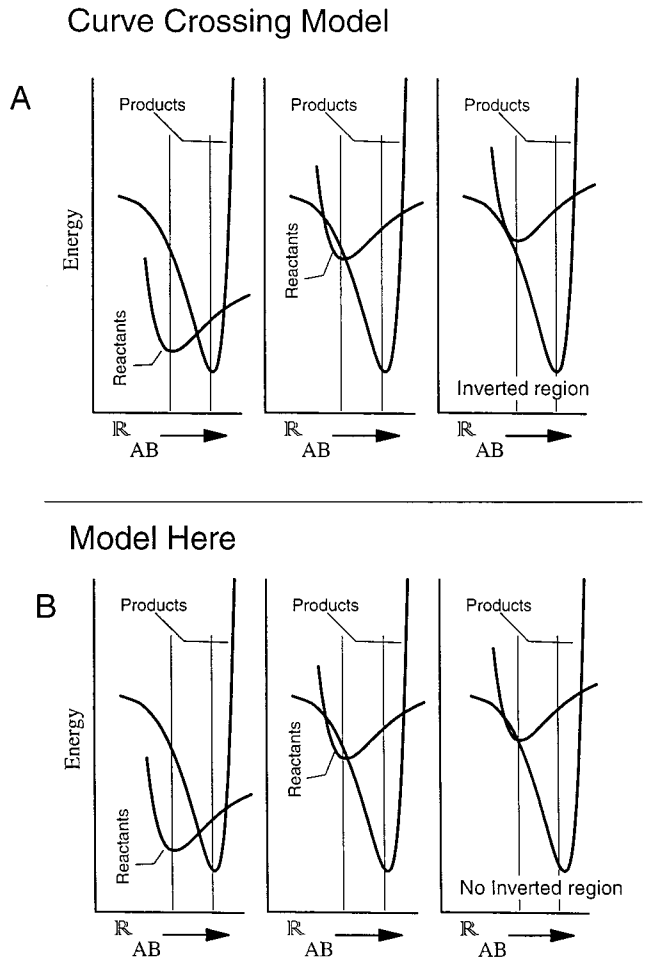

Figure 15. (a) Curve-crossing model in the inverted region. (b) The corresponding situation based on the model here.

reactions of the form

$$H + CH_3OH \rightarrow \text{products} \qquad (22)$$

Figure 16 shows how the activation energy correlates to the bond stretching energy and the Pauli repulsion energy. Notice that activation barriers correlate much better to the Pauli energy than to the bond stretching energy. Thus, the model here agrees with Blowers and Masel's ab initio calculations.

The model also agrees in principle with Shaik's valence bond model,[33−38] although there are some differences in detail. Overall, the model agrees quite well with data as can be seen in Figure 6.

VI. Summary

In summary then, the model here shows many of the trends one expects. If there are no Pauli repulsions, then there are no barriers to reactions. As one turns on the Pauli repulsions, the barriers increase. However, there is a nonlinear effect because the transition states become looser as the Pauli repulsions increase, and the transition states become tighter as the bond energy of the reactants increases. The tightening of the transition state produces an unexpected effect. In some cases, it is easier to break a strong bond than it is to break a weak bond. One can also get negative Brønsted coefficients in cases with reactivity where reaction 20 is slower than reaction 18, even though (CH_3)-$CHNO_2$ is a stronger acid than CH_3NO_2.

The model is virtually indistinguishable from the original Marcus equation when $-1 \leq \Delta H_r/4E_a^\circ \leq 1$. However, the

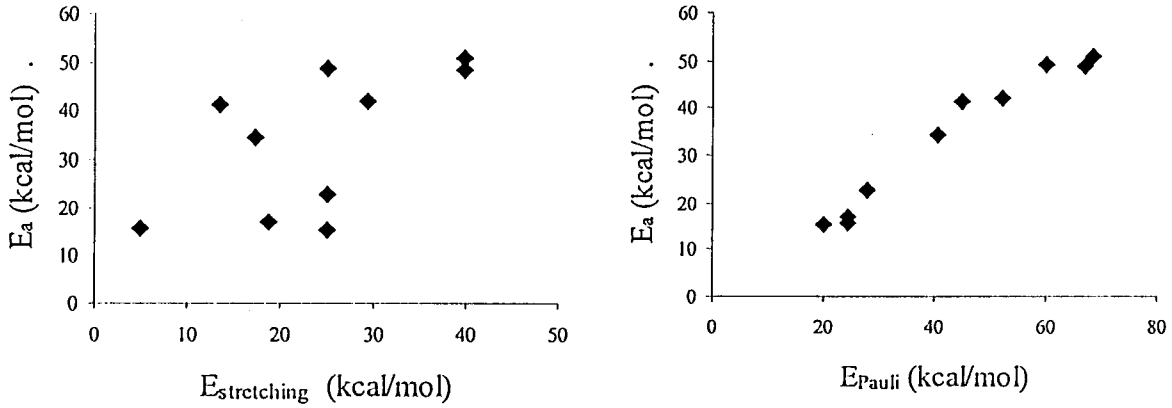

Figure 16. Activation energies for reactions of the form in eq 22 as a function of the Pauli energy and the bond stretching energy. Results of Blowers and Masel.[24,26]

model predicts that the activation barrier goes to zero for very exothermic reaction, approaches ΔH_r for very endothermic reaction, and varies nonlinearly in between. That trend seems to agree with experimental data, ab initio calculations, and Marcus' hyperbolic cosine equation. The model also predicts complex behavior with changing bond energy. Again, such a trend seems to agree with both data and ab initio calculations. In a larger way, the model suggests that the barriers to atom transfer reactions are mainly associated with the Pauli repulsions. In our previous ab initio calculations, we found that the barriers to reaction are negligible in the absence of Pauli repulsions and the magnitude of the barrier increases as the Pauli repulsions increase. In a larger way, the model seems to extend Marcus' original equation to very endothermic and very exothermic reactions.

Acknowledgment. This work was supported by NSF Grant CTS 96 10115. The authors also thank Dr. Rudolph Marcus for his helpful comments regarding this manuscript.

Supporting Information Available: Detailed derivations of eqs 11 and 13 and a table of the reactions considered in Figures 2 and 6. This material is available free of charge via the Internet at http://pubs.acs.org.

References and Notes

(1) Marcus, R. A. *J. Chem. Phys.* **1955**, *24*, 966.
(2) Marcus, R. A. *J. Chem. Phys.* **1968**, *72*, 891.
(3) Murdoch, J. R. *J. Am. Chem. Soc.* **1993**, *105*, 2667.
(4) Magnoli, D. E.; Murdoch, J. R. *J. Am. Chem. Soc.* **1981**, *103*, 7465.
(5) Chen, M. Y.; Murdoch, J. R. *J. Am. Chem. Soc.* **1989**, *108*, 4735.
(6) Shaik, S.; Schlegel, H. B.; Wolfe, S. *Theoretical Aspects of Physical Organic Chemistry*; Wiley & Sons: New York, 1992; p 37.
(7) Sutin, N. *Acc. Chem. Res.* **1968**, *1*, 57.
(8) Sutin, N. *Acc. Chem. Res.* **1983**, *30*, 441.
(9) Jensen, F. *J. Comput. Chem.* **1994**, *15*, 1199.
(10) Albery, W. J.; Kreevey, H. M. *Adv. Phys. Org. Chem.* **1978**, *16*, 87.
(11) Albery, W. J. *Electrode Kinetics*; Clarendon Press: Oxford, 1975.
(12) Evans, M. G.; Polanyi, M. *Trans. Faraday Soc.* **1938**, *34*, 11.
(13) Cohen, A. O.; Marcus, R. A. *J. Phys. Chem.* **1968**, *72*, 4249.
(14) Guthrie, J. P. *J. Am. Chem. Soc.* **1997**, *119*, 1151.
(15) Westley, F. *Table of Recommended Rate Constants for Chemical Reactions Occurring in Combustion*; U. S. Department of Commerce: Washington, DC, 1980.
(16) Benson, S. *Kinetic Data on Gas-Phase Molecular Reactions*; U. S. National Bureau of Standards: Washington, DC, 1970.
(17) Kondrat'ev, V. N. *Rate Constants of Gas-Phase Reactions*; Washington, DC, 1972.
(18) Lee, W. T.; Masel, R. I. *J. Phys. Chem.* **1998**, *102*, 2332.
(19) Lee, W. T.; Masel, R. I. *J. Phys. Chem.* **1996**, *100*, 10945.
(20) Polanyi, J. C.; Wong, W. H. *J. Chem. Phys.* **1969**, *51*, 1439.
(21) Polanyi, J. C. *Acc. Chem. Res.* **1972**, *5*, 161.
(22) Mok, M. H.; Polanyi, J. C. *J. Chem. Phys.* **1969**, *51*, 1451.
(23) Kuntz, P. J.; Nemeth, E. M.; Polanyi, J. C.; Rosner, S. D.; Young, C. E. *J. Chem. Phys.* **1966**, *44*, 1168.
(24) Blowers, P.; Ford, L.; Masel, R. I. *J. Phys. Chem, A.* **1998**, *102*, 9267.
(25) Blowers, P.; Masel, R. I. *Surf. Sci.* **1998**, *417*, 238.
(26) Blowers, P.; Masel, R. I. *J. Phys. Chem.* **1998**, *102*, 9957.
(27) Blowers, P.; Masel, R. I. *AIChE J.* **1999**, *45*, 1794.
(28) Bernstein, R. B.; Muckerman, J. T. *Adv. Chem. Phys.* **1967**, *12*, 393.
(29) Schatz, G. C. In *Potential Energy Surfaces and Dynamics Calculations*; Truhlar, D. G., Ed.; Plenum: New York, NY, 1981; p 287.
(30) Glukhovtsev, M. N.; Pross, A.; Radom, L. *J. Am. Chem. Soc.* **1995**, *117*, 2024.
(31) Glukhovtsev, M. N.; Pross, A.; Schlegel, H. B.; Bach, R. D.; Radom, L. *J. Am. Chem. Soc.* **1996**, *118*, 11258.
(32) Kresge, A. J. *Can. J. Chem.* **1974**, *52*, 1897.
(33) Shaik, S.; Hiberty, P. C. *Adv. Quantum Chem.* **1995**, *26*, 99.
(34) Shaik, S.; Hiberty, P. C. *J. Phys. Chem.* **1990**, *94*, 4089.
(35) Sastry, G. N.; Shaik, S. *J. Phys. Chem.* **1996**, *100*, 9794.
(36) Sastry, G. N.; Shaik, S. *J. Am. Chem. Soc.* **1995**, *117*, 3290.
(37) Shaik, S.; Shurki, A. *Angew. Chem.* **1998**, *38*, 587.
(38) Shurki, A.; Shaik, S. *THEOCHEM* **1998**, *424*, 37.